

Tribology Online

Vol. 20, No. 4 (2025) 166-178. ISSN 1881-2198 DOI 10.2474/trol.20.166

Japanese Society of Tribologists https://www.tribology.jp/trol/

Article

Tribochemical Manufacturing of Thin Functional Films on Silicon Oxide Surfaces

Khurshid Ahmad (b) 1)*, Alaaeddin Al Sheikh Omar¹⁾, Ajay Pratap Singh Lodhi¹⁾, Senbo Xiao²⁾, Chun Wang¹⁾, Krzysztof Kubiak¹⁾, Mark Wilson¹⁾, Jianying He²⁾, Zhiliang Zhang²⁾ and Ardian Morina¹⁾*

¹⁾ School of Mechanical Engineering, University of Leeds, Woodhouse Lane, Address One, Leeds, LS2 9JT, U.K.
²⁾ Department of Structural Engineering, Norwegian University of Science and Technology (NTNU),
Richard Birkelands Vei 1A, Trondheim, N-7491, Norway

*Corresponding author: Khurshid Ahmad (engrkhurshid@gmail.com) / Ardian Morina (a.morina@leeds.ac.uk)

Manuscript received 01 May 2025; accepted 11 September 2025; published 15 October 2025

Abstract

The discovery of tribochemical reactions at the sliding interfaces has suggested new pathways for material synthesis. This study explored the formation of thin functional films at the steel-on-silicon sliding interfaces, with toluene as base liquid and five different additives i.e. Zinc dialkyldithiophosphates (ZDDP), 3-Aminopropyltriethoxysilane (APTES), Octadecyltrimethoxysilane (OTMS), (3-mercaptopropyl) trimethoxysilane (MPTMS) and Octadecene. All additives were found to result in thin functional films of varying chemical, mechanical, and electrical characteristics. The Octadecene and OTMS APTES produced carbon rich tribofilms. The OTMS tribofilms were soft, as revealed by the quantitative nanomechanical analysis. The MPTMS and ZDDP additives resulted in conductive thin films in a well-defined linear pattern. The MPTMS resulted in continuous conductive films with surface coverage higher than that of the ZDDP.

Keywords

surface, tribochemical, thin films, wear

1 Introduction

Functional coatings have been developed for a wide range of applications. Various surface characteristics such as wettability [1, 2], conductivity [3], and mechanical strength [4] have been modified through such coatings. A wide range of its applications can be found in microelectromechanical and nanoelectromechanical systems (MEMS/NEMS). The MEMS/NEMS are fascinating developments that have further tremendous potential applications in automotive, biomedical, and advanced autonomous systems [5]. These devices range from sensors, actuators, micro-analysis to micro-optical systems, and bio-MEMS for surgeries. The MEMS are generally made with silicon wafers through a variety of methods such as chemical etching [6], photo lithography [7], micromachining [8], or deposition techniques [9]. Their surfaces are functionalized using various physical or chemical approaches such as chemical vapor deposition [10], spin coating [11, 12] and spray coating [13]. Continuous efforts have been made to find novel ways to produce MEMS and NEMS with desired functionalities, reliability, and durability. Tribo-based functionalization is one of such novel approaches that offers huge potential to address challenges in the manufacturing and desired functionality of devices. The tribo-based synthesis is attractive due to enhanced

control over the process compared to the traditional mechanochemical synthesis [14]. Unlike the negative connotation of material damage and of waste of energy associated with tribology, it offers an exciting direction for manufacturing of MEMS. The discovery of tribofilms at sliding interfaces [15] has suggested a new domain of looking into the use of tribology for producing thin functional films. Tribofilms are thin films that are formed at the sliding interfaces due to shear driven chemical reactions. A wider range of materials have been found to be forming tribofilms such as Zinc dithiophosphate (ZDDP) [16], dialkyldithiophosphate (DDP) [17], pyrrolidinium salts [18], ethanol [19], a variety of ionic liquid additives [20], and nanoparticles such as zirconia [21] and vanadium oxide [22].

Previously, tribofilms have been manufactured using multi asperity pin-on-plate tribometer [23], mini-traction machine [24], colloidal probe AFM [21] and single asperity sliding using AFM [25-27]. These studies have revealed that composite tribofilms can be grown to 3-D nanostructures, by using a mixture of ZDDP [28, 25, 27] or DDP [24] and base oil at controlled temperatures. For instance, Dorgham et al [25, 27] proposed that 3D patterning can be acquired using AFM probe. They were able to produce tribofilms thicker than 30 nm. Similarly, Khare et al [26] used AFM probe to produce 3D nanostructure with a mean height of more than 80 nm. In another study colloidal

probe was slid against the steel/silicon disc to study the Zirconia tribofilms [21]. Nucleation of tribofilms was observed with the volumetric growth increasing with the number of sliding cycles. A study conducted by Shirani et. al [19] found formation of 2D film of graphene on platinum coated gold surface, due to dissociation of ethanol at the sliding interface. Similarly, functional films with higher conductivity have been obtained by using mini-traction machine, through sliding a steel ball over silicon substrate immersed in Graphene-laden oil [3].

These studies propose a new direction for manufacturing and functionalization of surfaces. Unlike the thermal films, which are usually excellent choice for uniform surface coatings, the tribofilms could be used for films formation at selected location. The multilayered, conductive or high adhesion films formation with spatial selectivity makes it an emerging choice for MEMS manufacturing. Therefore, this study focused on exploring additive material for tribo-based manufacturing and functionalization which are compatible with silicon substrates. The goal was to identify alternative additives that can be used in liquid medium other than oil so that it could be used for MEMS and NEMS manufacturing applications. For this purpose, 06 different liquid mediums were selected i.e. only toluene, and toluene mixed with 10% (w/w) APTES, MPTMS, Octadecene, OTMS and ZDDP. The ZDDP was used for comparison purposes, as it has been used in previous studies [29, 17, 25]. The other additives were selected based on its compatibility with silicon wafers [30-34] and to explore its ability to form multilayer films or localized functionality such as enhanced conductivity. The tribofilms were analyzed using different analytical techniques to understand its chemical and physical characteristics. Molecular dynamic simulations were also run to obtain key insights into phenomena of interest.

2 Materials and methods

Materials:

The Zinc dithiophosphate were obtained from Afton Chemicals. While the 3-Aminopropyltriethoxysilane, Octadecyltrimethoxysilane, (3-mercaptopropyl) trimethoxysilane, Octadecene and Toluene were obtained from Sigma Aldrich). The Silicon Wafers with thin oxide film were obtained from Inseto UK. The Silicon wafer had Orientation: <111>, Resistivity: 1–10 ohm.cm with one side polished. The Roughness average (Ra) of the wafer was 0.07 nm. The pin was made of EN31 steel, with the surface roughness of 0.232 μm .

Methods:

A solution of 10% (w/w) the above-mentioned additives and Toluene was prepared. After adding the additives, the mixture was stirred using magnetic stirrer for 5 minutes at room temperature and 500 rpm. Fresh mixture was used for all experiments. Toluene was selected as solvent because of easy of cleaning and its excellent ability to disperse various additives including the organic silanes[1, 35-37]. The commercially available HiTEC1656 Performance Additive, secondary type ZDDP was used in this study. The aim was to identify alternatives that can be used in liquid medium other than oil so that it could be used for MEMS and NEMS manufacturing applications. The other additives were selected based on its compatibility with silicon wafers, [30-34] so that appropriate precursors could be identified for tribo based functionalization of surfaces. Silicon wafers were sliced into 1 cm² pieces. The cleaned sliced wafer was immersed in the solution by filling the mixture into the sample holder, mounted on the reciprocating

pin-on disc tribometer (TE77, Cameron Plint). Steel pins with 10 mm curvature radius were reciprocated over the silicon wafer using the pin-on-plate tribometer. The frequency was 3 Hz while the stroke length was 5 mm. Moreover, a normal load of 24.5 N was applied on the pin. The experimental conditions selected were in line with the published literature, so that the working in boundary region is ensured with less wear and favor the build-up at the sliding interface [29, 17, 25, 3, 38]. Each experiment was run for 30 min at room temperature.

Prior to use, the pins were cleaned with n-heptane for 20 minutes in the ultrasonic bath to remove the greasy material used for its anti-oxidation protection. Afterwards, they were cleaned in acetone for five minutes. The silicon wafers were cleaned with the help of commercially available "arco essentials" liquid detergents to remove contaminants from the substrates. The detergent contains 5-10% Anionic and <5% nonionic surfactants. The samples were thoroughly rinsed with copious DI water to remove the traces of detergents. Afterwards, the samples were sonicated for 5 minutes in acetone.

Surface Characterization:

The SEM (Carl Zeiss EVO MA15) equipped with the EDS was used for surface characterization and elemental analysis. Figure 1 shows the SEM images of the typical silicon wafer and pin used in these experiments. The topography, adhesion, deformation, and electrical conductivity were analyzed using AFM (Dimension Icon, Bruker, USA). AFM probe (NM-TC) with spring constant of 350 N/m and tip radius of 25 nm was used for the analysis. The peak force quantitative nanomechanical mapping (PFQM) was used to measure adhesion and deformation of the tribofilms. The PFQNM uses the Peak Force Tapping to measure the single point forces because of the tipsurface interactions while raster scanning the surface [39]. The scanning force (also known as peak force) that holds the tip against the surface in each tap, is adjusted through the tipsample distance by a feedback loop. The conductive AFM (CAFM) was used to analyze electrical conductivity. A voltage bias of 500 mV was used for the conductive AFM. Figure 2 shows the initial AFM analysis of the unused silicon wafer surface.

Molecular dynamic simulations:

Molecular dynamic simulations were used to understand the underlying mechanism of the formation of their tribofilms. A selected number of molecules were packed between two slabs of amorphous silica. The amorphous silica slabs were derived from cristobalite SiO₂ structure [40, 41]. The slab was heated from 300 K to 4000 K and then gradually cooled down to 300 K. All the simulations were performed at 300K. The specific temperature was chosen for MD simulations, in order to explore the effect of loading and shear only on the formation of new bonds between the additives and the sliding surfaces, thus avoiding the effect of temperature. The NVT ensemble was used with a heating and cooling rate of 0.02 K/fs. Avogadro 1.2 [42] and Moltemplate [43] were used for the construction of the model. In addition, Ovito [44] and Visual Molecular Dynamics (VMD) [45] were used for visualization and analysis of the radial distribution function. The pairwise interactions were modeled using Reaxff [46], while the force field parameters were taken from the study of Soria et al. [47]. The simulations were performed using a Large-scale Atomic / Molecular Massively Parallel Simulator (LAMMPS) [48]. The chosen Reaxff force is about to reproduce any chemical reaction, for example chemical bond formation, between the additives and the substrate, especially during the sliding under load. To study the reactions that can occur due to loading and sliding, a normal

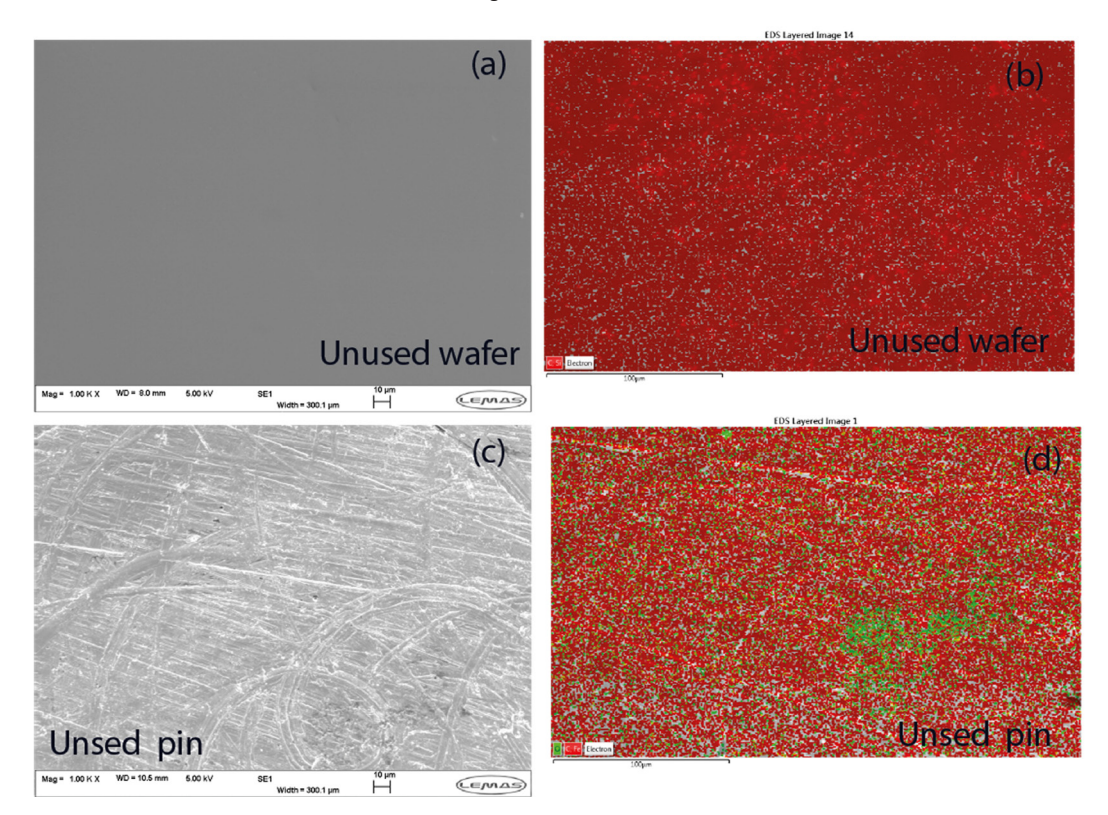


Fig. 1 SEM and EDS analysis of a typical unused silicon plate and pin (a) SEM image of unused silicon plate (b) EDS of unused silicon plate C-Si are shown in red color (c) SEM image of unused pin (d) EDS of unused pin C-Fe are shown in red color while O is shown in green

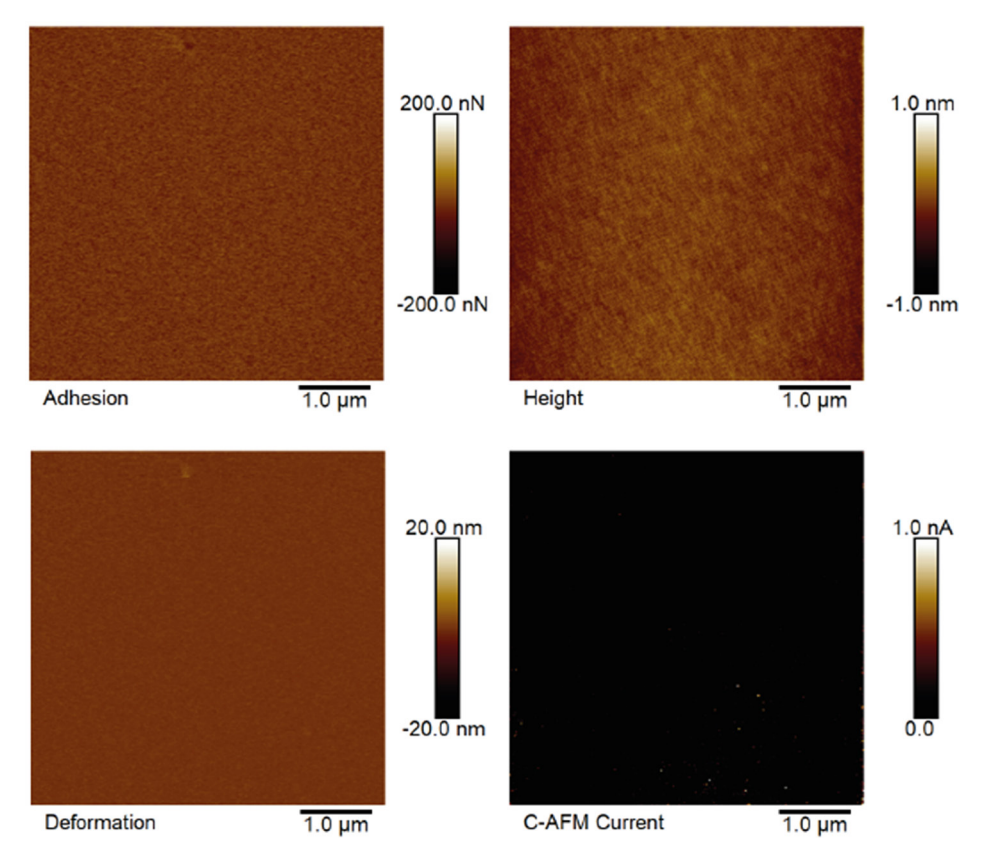


Fig. 2 AFM analysis of a typical silicon plate. The figure shows images of the measured adhesion, topography, deformation and current flow. It is clear from the results that the silicon plate is smooth and rigid while demonstrate low adhesion and low electrical conductivity.

load of 1 GPA was applied to the top atom layers of the $\rm SiO_2$ slab with thickness of 0.5 nm. This loaded layer was treated as a rigid body. The bottom layer of the lower slab with the same thickness was also treated as a wall. The APTES and MPTMS molecules were sheared between the top and bottom slabs, each moving with a velocity of 10 m/s in opposite directions. The simulations were run for approximately 1 ns, with simulation time step of 0.2 fs.

3 Results

3.1 Thin film surface analysis

The pins and silicon wafers were thoroughly analyzed with SEM and EDS to explore the thin film surface and composition. The SEM micrographs of pins and plates are shown in Figs. 3 and 4 respectively.

While the straight-line patterns are evident on the silicon wafer shown in Fig. 4, there is no evident wear pattern on the pins in Fig. 3. A build-up of additives material is also evident

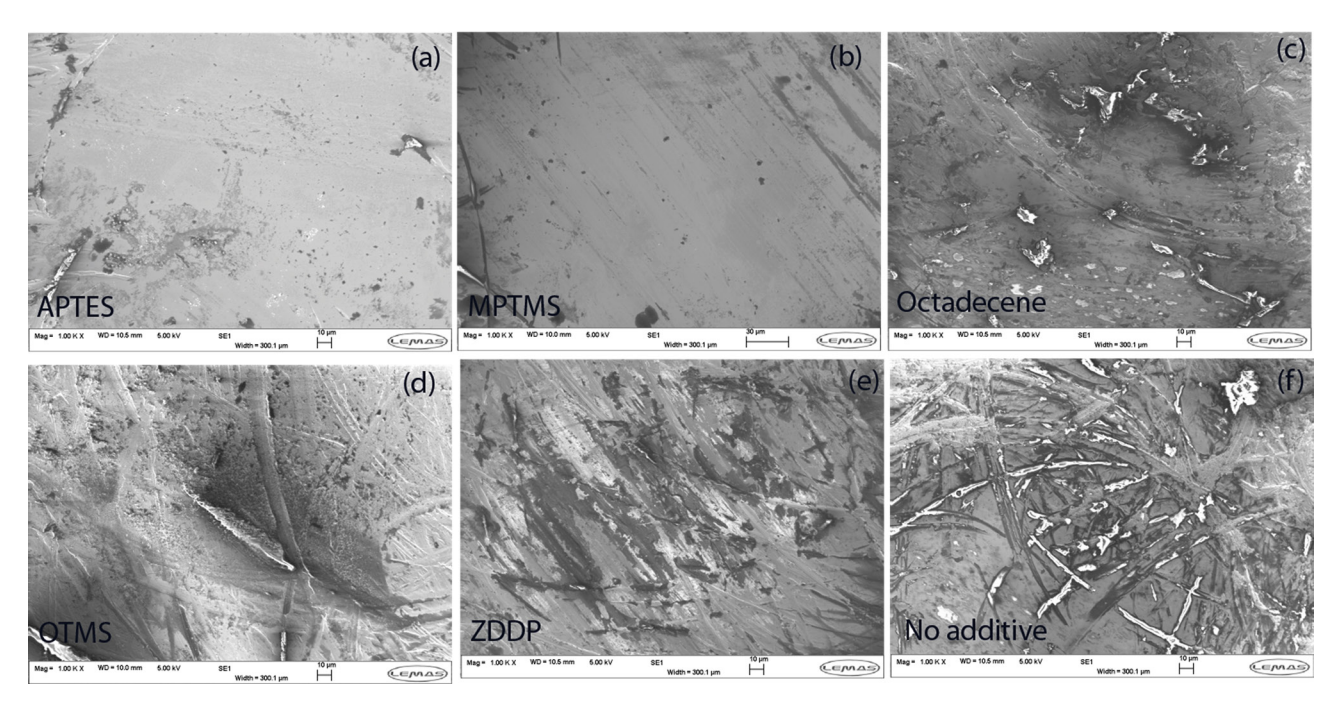


Fig. 3 SEM micrograph of steel pins used in the analysis (a) APTES (b) MPTMS (c) Octadecene (d) OTMS (e) ZDDP (f) Toleuene only. As evident from the micrograph, there are no clear signs of pin wear.

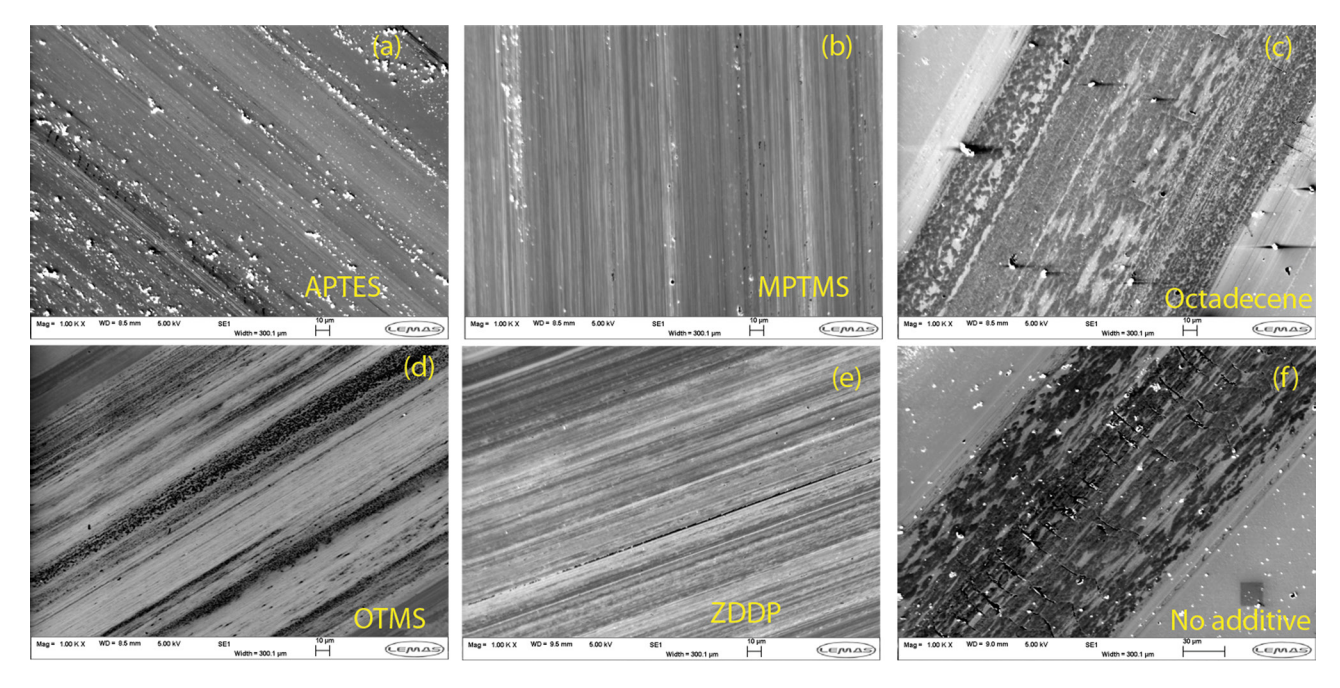


Fig. 4 SEM Images of the sliding track on the silicon wafers (a) APTES (b) MPTMS (c) Octadecene (d) OTMS (e) ZDDP (f) Toluene only. The micro-crakes are evident on the wafer where no additive was added.

from Fig. 3. Moreover, as shown in Fig. 4, except for the sample with no additives and Octadecene the other samples show continuous lines like pattern. Those two show micro-cracks, suggesting failure of the surface. The micro-cracks are more visible in the no-additive only toluene experiments. To answer the key questions such as, whether there is additive build-up on the pins surface and if there is any thin film formed on the silicon surface, the elemental analysis of the pins and plates was performed with the help of EDS. A comparison of EDS mapping is given in Figs. 5 and 6.

The higher concentration of silicon in the sliding track of APTES samples in Fig. 6, gives an indication of build-up. The coexistence of silicon-carbon in MPTMS, Octadecene, OTMS and ZDDP samples suggests formation of carbon-silicon rich composite films. The presence of Fe in the only toluene sample suggests material transfer from the pin to the wafer, giving a strong indication of abrasive wear at the interface. For a more in-depth comparison, the single-point elemental analysis was performed within and outside the sliding track. The results are shown in Tables 1 and 2. Where Table 1 data has been obtained

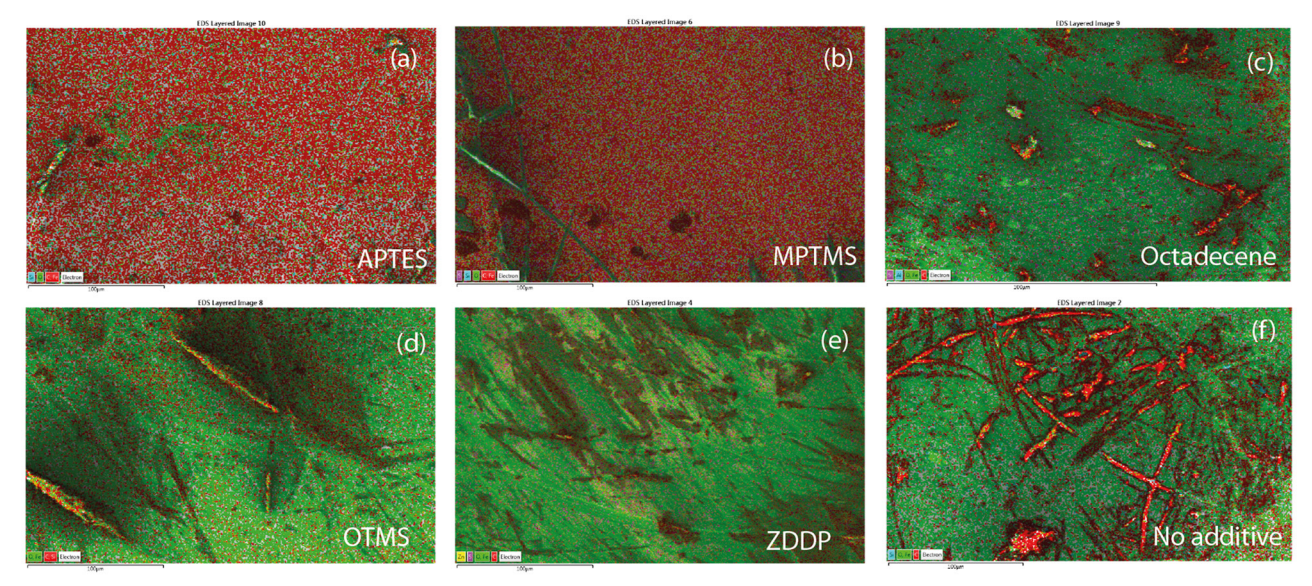


Fig. 5 EDS analysis of the steel pins after the test (a) APTES - sky blue and green show Si and O respectively, while red shows C and Fe (b) MPTMS -purple, sky blue and green show S, Si, and O respectively while red shows C and Fe (c) Octadecene - purple, sky blue and red show Si, Al, and C respectively while green shows O and Fe (d) OTMS - Green shows Fe, and O while red shows C and Si (e) ZDDP - yellow, purple and red show Zn, S and C respectively, while green shows O and Fe (f) Toluene only - sky blue and red show Si and C respectively while green shows O and Fe. The variation in the constituents of the tribofilms on the pins is evident from the images.

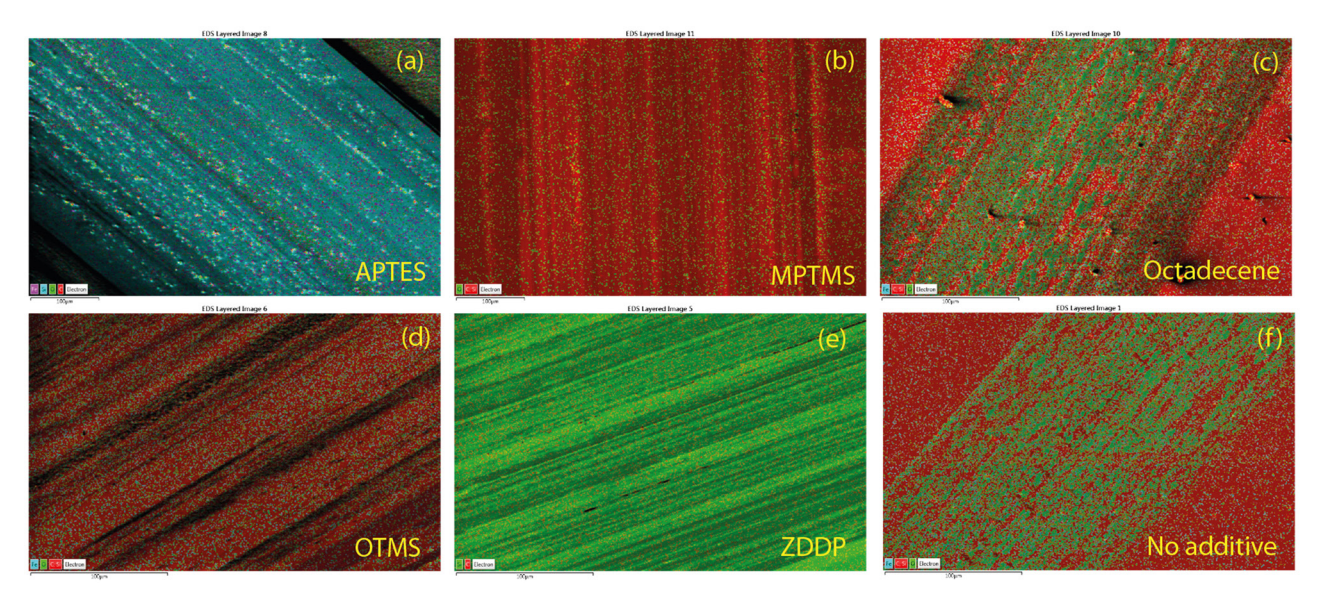


Fig. 6 EDS analysis of the silicon wafers after the test (a) APTES - purple, sky blue, green and red show Fe, Si, O and C respectively (b) MPTMS - green shows O while red shows Si and C (c) Octadecene - sky blue and Green show Fe, and O respectively, while red shows C and Si (d) OTMS - sky blue and Green show Fe, and O respectively, while red shows C and Si (e) ZDDP - green and red show Si and C respectively (f) Toluene only - sky blue and Green show Fe, and O respectively. The variation in the constituents of the tribofilms is evident from the images.

Table 1 EDS analysis of steel pins used in the analysis

Element	Unused Pin (mass%)	Toluene Only (mass%)	ZDDP (mass%)	MPTMS (mass%)	Octadecene (mass%)	OTMS (mass%)	APTES (mass%)
С	3.43	48.28	12.06	32.07	65.59	36.3	22.67
О	1.53	3.42	2.93	1.65	6.15	27.73	13.84
Si	-	0.57	1.8	0.34	0.92	20.49	9.49
P	-	-	2.33	-	-	-	
S	-	-	3.27	0.84	-	-	_
N	-	-	_	-	_	-	2.92
Zn	-	-	5.43	-	_	-	
Fe	93.01	46.84	72.18	65.1	26.81	15.47	51.08
Al	0.46	-	_	-	0.52	-	_
W	1.56	0.88	-	-	_	-	_
Total:	100	100	100	100	100	100	100

Table 2 EDS point analysis of the sliding track on silicon surface, after sliding experiments

Element	Unused wafer (mass%)	Toluene Only (mass%)	ZDDP (mass%)	MPTMS (mass%)	Octadecene (mass%)	OTMS (mass%)	APTES (mass%)
С	1.84	8.72	2.74	2.68	3.15	4.29	3.08
Ο	0.31	12.53	0.46	0.53	6.17	2.4	2.36
Si	97.85	62.79	96.8	96.79	82.85	91.59	91.93
Fe	-	15.97	_	_	7.83	1.72	2.62
Total:	100	100	100	100	100	100	100

from the analysis of Si wafer while that of Table 2 from pin.

The pins provided interesting evidence in support of the formation and presence of thin tribofilms. For example, the higher percentages of carbon on all pins, as opposed to the unused pin, reinforced the deduction that tribofilms have formed during the sliding process. Generally, higher percentages of Silicon and Oxygen or Carbon were observed on pins where additives were used, in addition to higher percentages of Carbon on the pins used for toluene-only experiments. For ZDDP, Zinc, Sulfur, and Phosphorus confirmed the formation of the Tribofilms, while for MPTMS, the presence of sulfur gave a strong indication of the presence of tribofilms. The silicon wafers, on the other hand, also suggested the formation of tribofilms, as evidenced in Table 2. Interestingly, the presence of higher concentration of carbon in the sliding track on the sample without any additives suggests the tribo-cracking of toluene. Previously, a similar phenomenon has been reported for ethanol, where 2D carbon films were formed due to splitting of carbon bonds and successive deposition over the platinum coated gold surface [19]. The results confirm the existence of the constituents of the additives on both surfaces, strongly suggesting the formation of tribofilms. The reduction in the traces of iron as compared to the only toluene sample, is a further indication of the existence of the protective layers, that reduced the material transfer from the pin to the surface.

To know more about the functional characteristics of thin films, the plates were analyzed with the help of Peak Force QNM and conductive AFM. The results are discussed as follows.

3.2 Functional characteristics of the films

The functional characteristics were analyzed with the help of AFM. For the mechanical characteristics such as adhesion and deformation the peak force QNM was used. The adhesion scans are given in Fig. 7. The adhesion varied on all samples with reference to unused silicon samples. A comparably higher variation in adhesion was observed on all samples except APTES and the unused silicon wafer. This could be attributed to the variation in the chemical topography, composition, and deformability. Therefore, the topography and the deformability (indicating how soft the films are) of the films were analyzed as shown in Figs. 8 and 9, respectively. It is evident from Fig. 8 that the surfaces with larger peaks and valleys show higher adhesion. This could be attributed to the larger tipsample contact area due to the roughness. The analysis of the deformability of the films showed that OTMS is more deformable than the rest of the materials. Suggesting soft nature of the films The deformation varied at different locations on OTMS, Octadecene, ZDDP and only toluene samples. The electrical conductivity of the samples was also analyzed using conductive AFM technique, as shown in Fig. 10. The results shown in Fig. 10 illustrate that the OTMS and Octadecene

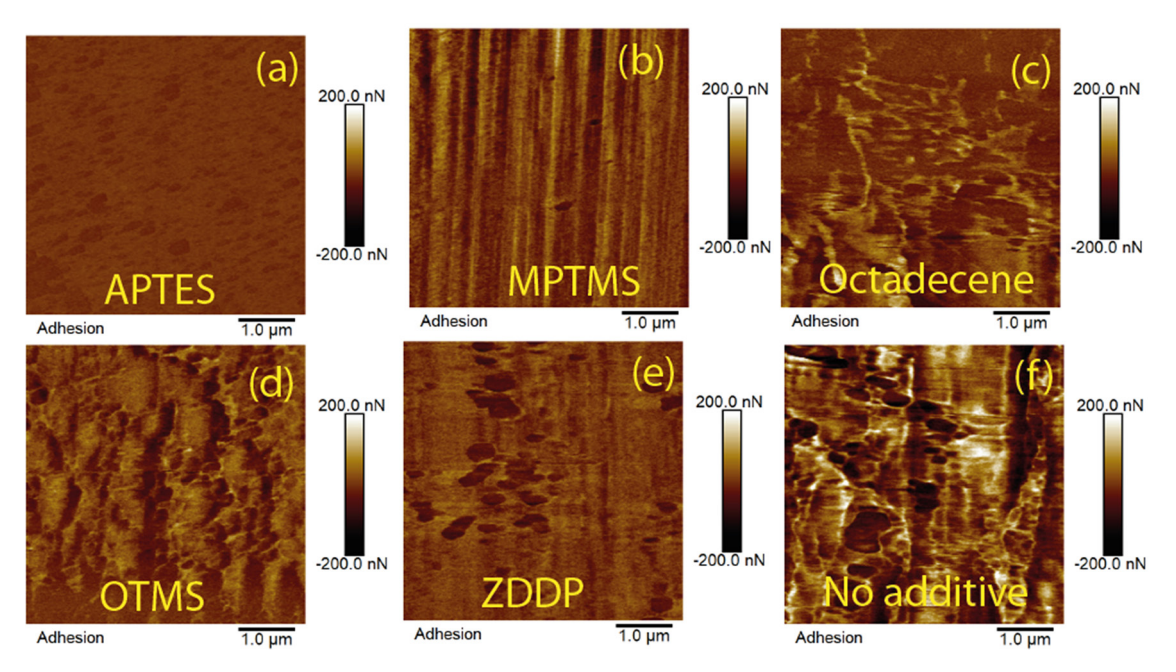


Fig. 7 Illustration of the variation in the adhesion on the tribofilm samples, obtained through the PF-QNM mapping(a) APTES (b) MPTMS (c) Octadecene (d) OTMS (e) ZDDP (f) Toluene only. The variation in the adhesion is evident across all sample.

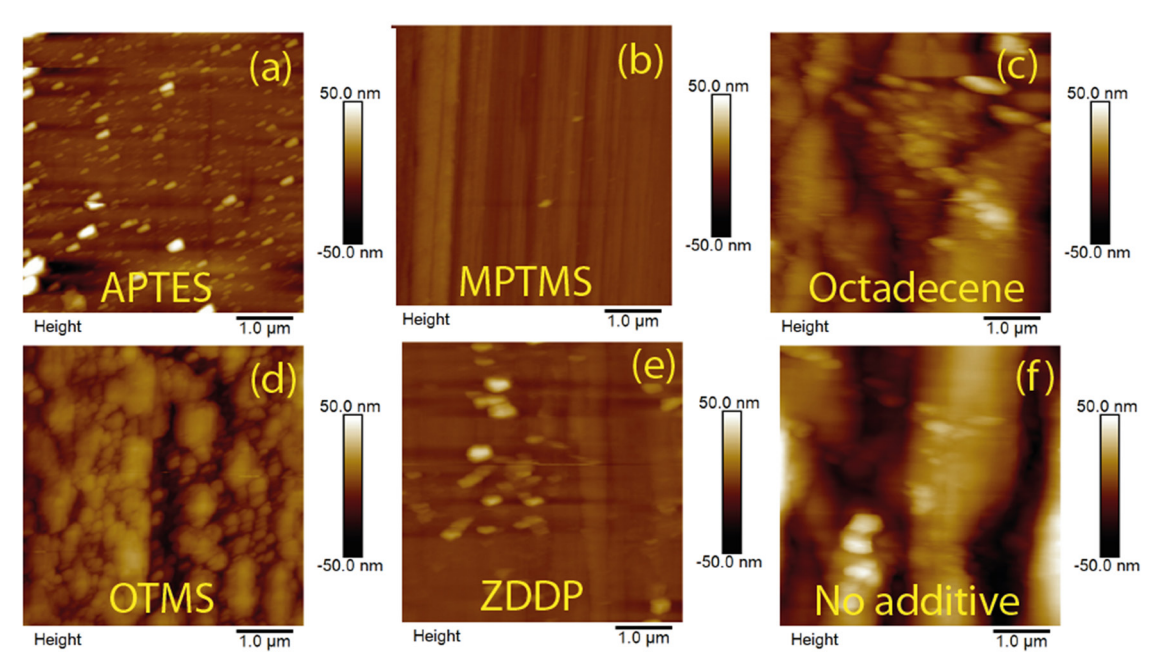


Fig. 8 AFM height images of tribofilm samples (a) APTES (b) MPTMS (c) Octadecene (d) OTMS (e) ZDDP (f) Toleuene only. The variation in the topography is evident.

samples are like the bare silicon sample in terms of current flow. The low current flow suggests lower electrical conductivity. The toluene-only sample had some areas that were relatively more conductive as compared to the bare silicon sample, which could be attributed to the presence of higher carbon concentration because of the tribochemical process during the experiments. However, MPTMS, ZDDP, and APTES resulted in tribofilms that were conductive. Among these three, the MPTMS resulted in considerably higher electrical conductivity of the films, whereas the APTES and ZDDP had some areas that exhibited a higher current flow. Previously, a lower conductivity has been reported for ZDDP [3], which is aligned with the current study

as the conductivity of the film did not vary uniformly over the entire scan area. The conductive films of the MPTMS on the other hand were continuous as evident from the Fig. 10. This could be attributed to the formation of conductive films during the tribo process, which could be formed due to the cracking of the additives [19]. The film thickness was analyzed with the help of profilometry, AFM and ellipsometry.

The results suggested film thickness of more than 100 nm for the APTES while less than 1 nm for the MPTMS and the ZDDP. While the thickness of the OTMS, Octadecene and Toluene-only samples was difficult to estimate due to the roughness of the surfaces. The APTES also resulted in 3D

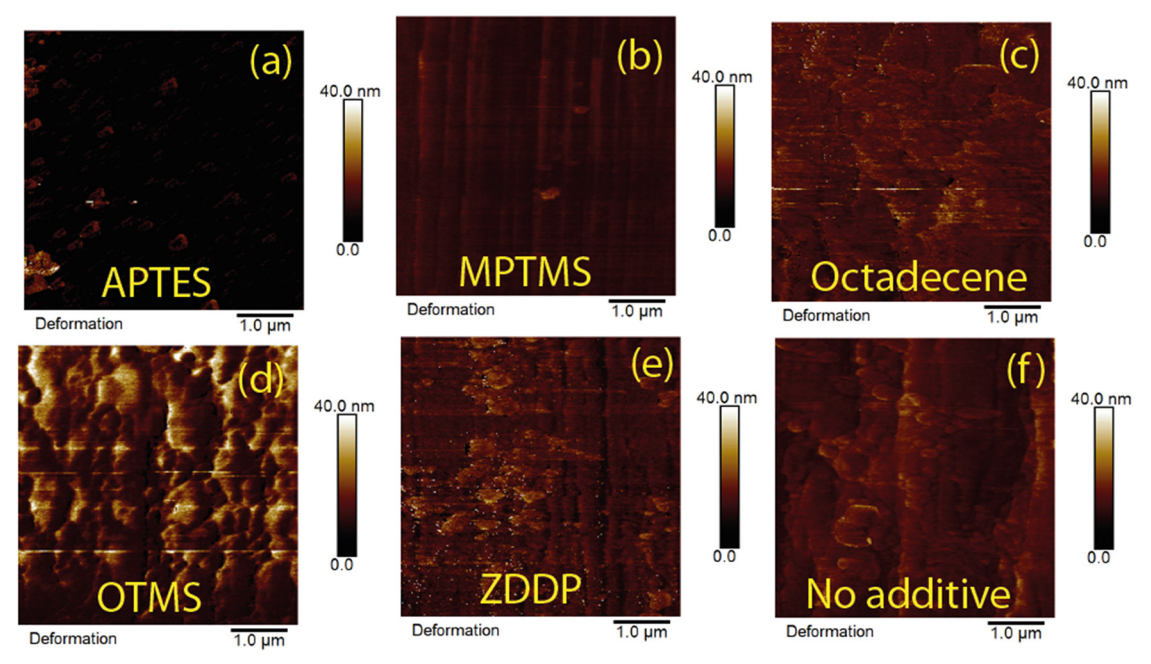


Fig. 9 Illustration of the variation in the deformation of the tribofilm samples, obtained through the PF-QNM mapping (a) APTES (b) MPTMS (c) Octadecene (d) OTMS (e) ZDDP (f) Toleuene only. The variation in the deformation can be easily observed over each sample as well as with respect to each other.

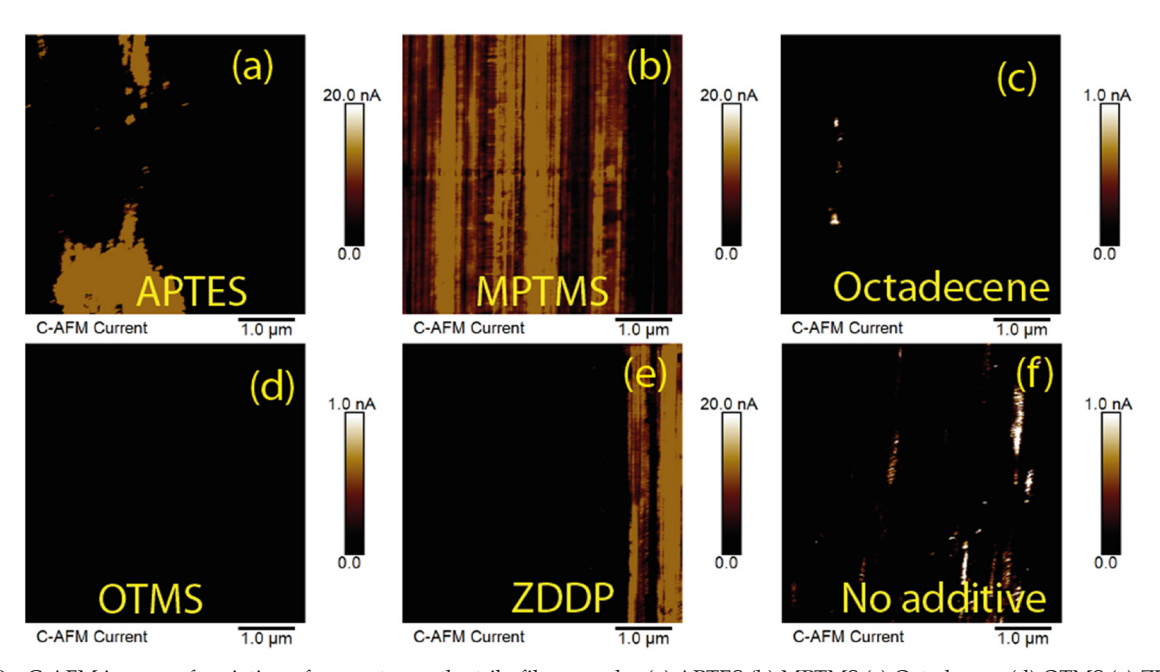


Fig. 10 C-AFM images of variation of current over the tribofilm samples (a) APTES (b) MPTMS (c) Octadecene (d) OTMS (e) ZDDP (f) Toluene only. Higher current values suggest higher electrical conductivity in the regions.

film which wasn't demonstrated by the rest of the additives. The surface profilometry and AFM images of a typical APTES sample are shown in Figs. A1 and A2 of the Appendix (supporting information). While the ellipsometry curves for uncoated silicon, ZDDP and MPTMS samples are shown in Fig. A4 of the Appendix (supporting information).

3.3 Molecular dynamic simulations of APTES and MPTMS films formation

As evident from the previous discussion, APTES and

MPTMS resulted in tribofilms with phenomenal characteristics. The APTES resulted in thicker films. While the MPTMS resulted in conductive films with higher coverage and continuity. Therefore, molecular dynamic simulations were used to understand the underlying mechanism of the formation of these films. For this purpose 25 APTES and 34 MPTMS molecules were packed between two amorphous silica slabs. The schematic of a typical simulation system is shown in Fig. 11.

The radial distribution functions were calculated to explore whether any new bonds were formed between the

APTES/MPTMS molecules and the silica slabs. The C-O radial distribution function for both molecules and the silica slabs is shown in Fig. 12.

A peak is clearly visible at distance of 1.2 Angstrom, both under loading and sliding. Particularly, the peak of radial distribution function during sliding increase significantly during the sliding simulations, which suggest the formation of new bonds between the carbon from APTES and MPTMS molecules and the oxygen from the silica slab.

4 Discussion

Silicon wafers were functionalized with thin composite films using tribo-based technique. Five different additives were dispersed in toluene to study their ability to form thin functional films on silicon plates. Toluene was used because it can be easily cleaned as compared to base-oil. It is also an excellent dispersant, used for dispersion of additives [37]. The additive materials are known to be forming self-assembled layers [49, 50], agglomerates [51] and chemical bonding to the surfaces through mechanochemical process [33]. As evident from the results of the molecular dynamic simulations, the C-S bonds in the MPTMS breaks which lead to the attachment of the fragments to the silicon or pin surface as evidenced by the build-

up on the pin surface. The APTES on the other hand caused a build-up, with thickness of more than 100 nm. This is likely to be caused by the ability of APTES to form multiple layers [52] and possible multiple configurations of interacting with the surfaces [34]. Another mechanism is due to the breakage of the C-N bonds, which is likely to be the case as evidenced by the absence of Nitrogen in the EDS analysis of the silicon surfaces and molecular dynamic simulations. The difference in the ability of the two materials to build up a thin or thicker film is likely due to the structure of the two polymers. Also structure and steric hindrances [53, 54] can cause different surface coverage and deposition. The variation in the adhesion over each sample as well as with each other can be attributed to the composition [55], contact mechanism [56, 57] and deformation [58] of the films. The variations are evident from Figs. 4, 8 and 9, across all samples. For example, the chemical composition on the samples vary with respect to each other as shown in Table 2. Similarly, the topographic changes in Fig. 8 suggests variation in the tip sample contact area over the sample. Moreover, the deformation analysis suggests that the adhesion is higher on the deformable surfaces, as evident from the deformation of the OTMS in Fig. 9.

It is also relevant to mention that during the sliding process wear of the surface occurs inevitably. Therefore, wear and surface morphological changes occurred since there is an

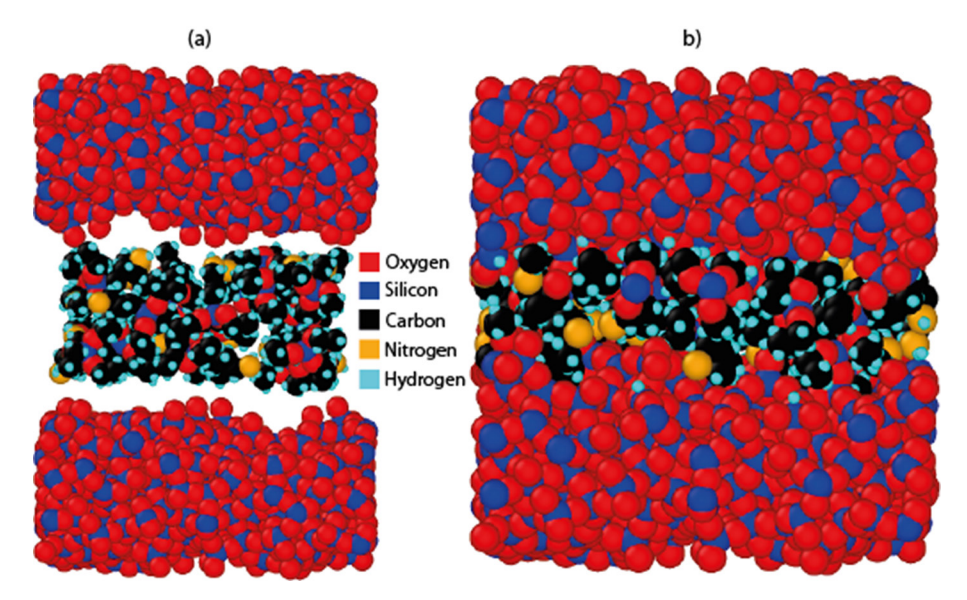


Fig. 11 Schematic of the molecular modeling of APTES. (a) Schematic of molecular arrangements before loading (b) Snapshot of the molecular system after applying 1 GPa load on the top slab.

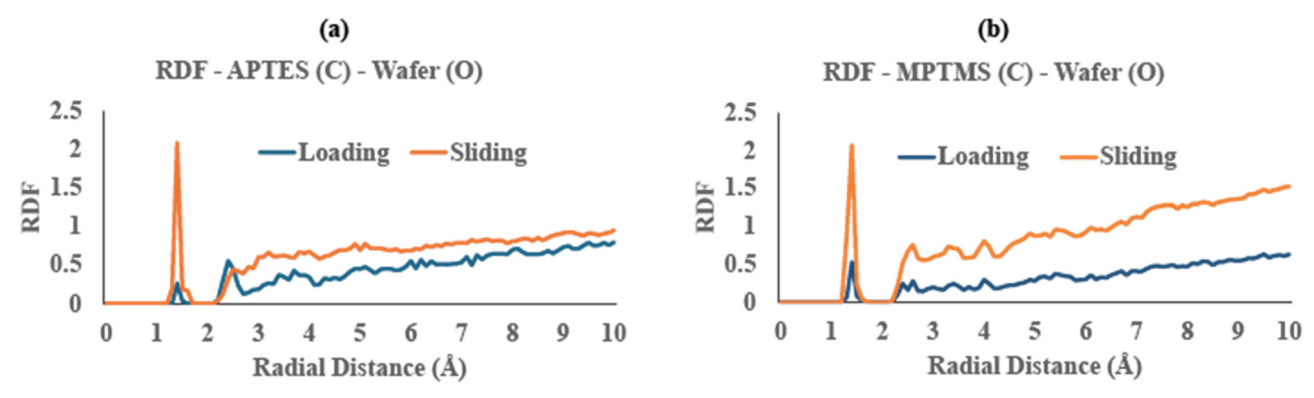


Fig. 12 Radial distribution function plots of the C-O from additive and wafer, respectively (a) APTES (b) MPTMS

induction time for the formation of tribofilm by each of the additives. The results in Fig. 4 suggest an evident abrasive wear on the Toluene-only sample which led to formation of microcracks. Such wear is undoubtedly detrimental to the surface and material, thus undesirable. However, the additives proved to be effective in protecting the surfaces from further wear and also imparted functional characteristics to the surface. This is clear from the results, especially, the APTES, where the additives resulted in a 3D nano-film at the interface. The morphological changes can affect the contact mechanics, friction and adhesion [59], however, whether the change would be positive or negative depends on the overall MEMS system.

The results evidenced unique characteristics with reference to the morphological changes. Such as the APTES resulted in low adhesion and comparatively smooth surfaces. Apart from that it resulted in the formation of a 3D film at the sliding interface. This suggested that the APTES can be used for manufacturing or spatially selected 3D features. Similarly, the MPTMS resulted in relatively higher conductivity films which suggested its potential use for selective functionalization of MEMS surfaces. The irregular MEMS surface can affect the contact behavior [59, 60] and therefore, it is highly dependent on the overall system, when the MEMS parts, surfaces and interfaces are interacting with each other. The electrical conductivity analysis suggests comparatively higher conductivity of the samples such as APTES, ZDDP and MPTMS. While the effect of removal of the thin oxide layer on the silicon wafer, as a result of the surface wear could contribute to the conductivity changes, it is likely that the higher conductivity may be due to the formation conductive thin films which have been reported previously to be forming at the sliding interfaces in organic medium [3, 19]. Moreover, it is also suggested by the molecular dynamic simulations that upon breakage of the carbon-sulfur or carbon-nitrogen bonds, new C-O bonds are formed. Therefore, it is likely that a conductive composite film of C, Si and O is formed at the sliding interfaces.

5 Conclusion

This study reports the manufacturing of thin functional films of ZDDP, APTES, OTMS, MPTMS and Octadecene, added into toluene. It was found that all additives result in thin films of varying characteristics. Such as the OTMS resulted in soft films while the APTES resulted in thicker films. The Toluene and Octadecene resulted in carbon rich composite nonconductive films. However, the films of the APTES and ZDDP had conductive patches with partial coverage. The MPTMS on the other hand resulted in continuous conductive films with comparatively higher surface coverage. This is likely to be the result of the formation of conductive composite layer at the sliding interface. The results suggested that the constituents and structures of the additives play an important role in the thickness and nature of the tribofilms.

Acknowledgement

All authors acknowledge the support of EPSRC under the Tribology as Enabling Technology (TRENT) Grant [Grant Number EP/S030476/1]. The authors also acknowledge the support of Leeds Electron Microscopy and Spectroscopy Centre, University of Leeds Research Computing for access to the High Performance Computing facilities and Bragg Centre for Materials Research for ellipsometry.

References

- Ahmad K, Zhao X, Pan Y. Effect of surface morphology on measurement and interpretation of boundary slip on superhydrophobic surfaces. Surface and Interface Analysis. 2017;49: 594–598
- [2] Ahmad K, Ahmad AS, Hassan M, Ahmad Z, Zhao X, Pan Y. Analysis of liquid mediated contact of glass colloidal particle with polystyrene coated surface. Surface Review and Letters. 2020;27: 1950101.
- [3] Duston S, Oliver R, Kubiak K, Wang Y, Wang C, Morina A. Tribological manufacturing of ZDDP tribofilms functionalised by graphene nanoplatelets. Journal of Physics: Materials. 2024;7: 045001.
- [4] Yang L, Neville A, Brown A, Ransom P, Morina A. Friction reduction mechanisms in boundary lubricated W-doped DLC coatings. Tribology International. 2014;70: 26–33.
- [5] Crone WC, Sharpe WN. A brief introduction to MEMS and NEMS. Springer New York, NY, USA. 2008: 203–228.
- [6] Pal P, Swarnalatha V, Rao AVN, Pandey AK, Tanaka H, Sato K. High speed silicon wet anisotropic etching for applications in bulk micromachining: A review. Micro and Nano Systems Letters. 2021;9: 1–59.
- [7] Lall J, Zappe H. MEMS-compatible structuring of liquid crystal network actuators using maskless photolithography. Smart Materials and Structures. 2022;31: 115014.
- [8] Mehregany M, Zorman CA, Roy S, Fleischman AJ, Rajan N. Silicon carbide for microelectromechanical systems. International Materials Reviews. 2000;45: 85–108.
- [9] Teh KS, Cheng YT, Lin L. MEMS fabrication based on nickelnanocomposite: film deposition and characterization. Journal of Micromechanics and Microengineering, 2005;15: 2205.
- [10] Hankins MG, Resnick PJ, Clews PJ, Mayer TM, Wheeler DR, Tanner DM, Plass RA. Vapor deposition of amino-functionalized self-assembled monolayers on MEMS. Reliability, Testing, and Characterization of MEMS/MOEMS II. SPIE. 2003;4980: 238–247.
- [11] Doms M, Feindt H, Kuipers W, Shewtanasoontorn D, Matar A, Brinkhues S, Welton R, Mueller J. Hydrophobic coatings for MEMS applications. Journal of Micromechanics and Microengineering. 2008;18: 055030.
- [12] Ahmad K, Zhao X, Pan Y, Hussain D. Characterization of spherical domains at the polystyrene thin film-water interface. Beilstein Journal of Nanotechnology. 2016;7: 581–590.
- [13] Yong Yeow L, Liming Y, Francis E. Characterization of spray coating photoresist for MEMS applications. Science and Technology. 2005;8: 383–390.
- [14] Carlton H, Huitink D, Liang H. Tribochemistry as an alternative synthesis pathway. Lubricants. 2020;8: 87.
- [15] Spikes H. The history and mechanisms of ZDDP. Tribology Letters. 2004;17: 469–489.
- [16] Zhang J, Spikes H. On the mechanism of ZDDP antiwear film formation. Tribology Letters. 2016;63: 1–15.
- [17] Dorgham A, Azam A, Parsaeian P, Wang C, Morina A, Neville A. Nanoscale viscosity of triboreactive interfaces. Nano Energy. 2021-79: 105447
- [18] Otero I, Lopez ER, Reichelt M, Fernandez J. Tribo-chemical reactions of anion in pyrrolidinium salts for steel–steel contact. Tribology International. 2014;77: 160–170.
- [19] Shirani A, Li Y, Smith J, Curry JF, Lu P, Wilson M, Chandross M, Argibay N, Berman D. Mechanochemically driven formation of protective carbon films from ethanol environment. Materials Today Chemistry. 2022;26: 101112.
- [20] Zhou Y, Qu J. Ionic liquids as lubricant additives: A review. ACS Applied Materials & Interfaces. 2017;9: 3209–3222.
- [21] Khare HS, Lahouij I, Jackson A, Feng G, Chen Z, Cooper GD,

- Carpick RW. Nanoscale generation of robust solid films from liquiddispersed nanoparticles via in situ atomic force microscopy: Growth kinetics and nanomechanical properties. ACS Applied Materials & Interfaces. 2018;10: 40335–40347.
- [22] Straiton AJ, Kathyola TA, Sweeney C, Parish JD, Willneff EA, Schroeder SL, Morina A, Neville A, Smith JJ, Johnson AL. Green alternatives to zinc dialkyldithiophosphates: Vanadium oxide-based additives. ACS Applied Engineering Materials. 2023;1: 2916–2925.
- [23] Al Sheikh Omar A, Salehi FM, Farooq U, Morina A. Additives depletion by water contamination and its influences on engine oil performance. Tribology Letters. 2024;72: 74.
- [24] Dorgham A, Parsaeian P, Azam A, Wang C, Ignatyev K, Mosselmans F, Morina A, Neville A. Tribochemistry evolution of DDP tribofilms over time using in-situ synchrotron XAS. Tribology International. 2021:60: 107026.
- [25] Dorgham A, Parsaeian P, Azam A, Wang C, Morina A, Neville A. Single-asperity study of the reaction kinetics of P-based triboreactive films. Tribology International. 2019;133: 288–296.
- [26] Khare H, Gosvami N, Lahouij I, Milne Z, McClimon J, Carpick RW. Nanotribological printing: A nanoscale additive manufacturing method. Nano Letters. 2018;18: 6756–6763.
- [27] Dorgham A, Wang C, Morina A, Neville A. 3D Tribo-nanoprinting using triboreactive materials. Nanotechnology. 2019;30: 095302.
- [28] Ueda M, Kadiric A, Spikes H. ZDDP tribofilm formation on nonferrous surfaces. Tribology Online. 2020;15: 318–331.
- [29] Al Sheikh Omar A, Ahmad K, Lodhi APS, Wang C, Kubiak K, Morina A. APTES nanofilm manufacturing using sliding interfaces. Proceedings of the Institution of Mechanical Engineers, Part J: Journal of Engineering Tribology. 2025;239: 1246–1257.
- [30] Amrute AP, Zibrowius B, Schüth F. Mechanochemical grafting: A solvent-less highly efficient method for the synthesis of hybrid inorganic-organic materials. Chemistry of Materials. 2020;32: 4699– 4706.
- [31] Gothe PK, Gaur D, Achanta VG. MPTMS self-assembled monolayer deposition for ultra-thin gold films for plasmonics. Journal of Physics Communications. 2018;2: 035005.
- [32] Ray SS, Chen S-S, Chang H-M, Thanh CND, Le HQ, Nguyen NC. Enhanced desalination using a three-layer OTMS based superhydrophobic membrane for a membrane distillation process. RSC Advances. 2018;8: 9640–9650.
- [33] Wacaser BA, Maughan MJ, Mowat IA, Niederhauser TL, Linford MR, Davis RC. Chemomechanical surface patterning and functionalization of silicon surfaces using an atomic force microscope. Applied Physics Letters. 2003;82: 808–810.
- [34] Wolf NR, Yuan X, Hassani H, Milos F, Mayer D, Breuer U, Offenhäusser A, Wördenweber R. Surface functionalization of platinum electrodes with APTES for bioelectronic applications. ACS Applied Bio Materials. 2020;3: 7113–7121.
- [35] Li Y, Bhushan B. The effect of surface charge on the boundary slip of various oleophilic/phobic surfaces immersed in liquids. Soft Matter. 2015;11: 7680–7695.
- [36] McGovern ME, Kallury KM, Thompson M. Role of solvent on the silanization of glass with octadecyltrichlorosilane. Langmuir. 1994:10: 3607–3614.
- [37] Mello VS, Faria EA, Alves SM, Scandian C. Enhancing Cuo nanolubricant performance using dispersing agents. Tribology International. 2020;150: 106338.
- [38] Yuan Y, Wang C, Lee S, Wilson MC, Morina A. Evaluation of nanoparticles for nanoscale film fabrication harnessing tribochemistry. Tribology International. 2025;210: 110805.
- [39] Pittenger B, Erina N, Su C. Mechanical property mapping at the nanoscale using peakforce QNM scanning probe technique. Nanomechanical Analysis of High Performance Materials. Springer.

- 2013: 31-51.
- [40] Khajeh A, He X, Yeon J, Kim SH, Martini A. Mechanochemical association reaction of interfacial molecules driven by shear. Langmuir. 2018;34: 5971–5977.
- [41] Stachurski ZH. On structure and properties of amorphous materials. Materials. 2011;4: 1564–1598.
- [42] Hanwell MD, Curtis DE, Lonie DC, Vandermeersch T, Zurek E, Hutchison GR. Avogadro: An advanced semantic chemical editor, visualization, and analysis platform. Journal of Cheminformatics. 2012:4: 1–17.
- [43] Jewett AI, Zhuang Z, Shea J-E. Moltemplate a coarse-grained model assembly tool. Biophysical Journal. 2013;104: 169A.
- [44] Stukowski A. Visualization and analysis of atomistic simulation data with OVITO–the open visualization tool. Modelling and Simulation in Materials Science and Engineering, 2009;18: 015012.
- [45] Humphrey W, Dalke A, Schulten K. VMD: Visual molecular dynamics. Journal of Molecular Graphics. 1996;14: 33–38.
- [46] van Duin AC, Dasgupta S, Lorant F, Goddard WA. ReaxFF: A reactive force field for hydrocarbons. The Journal of Physical Chemistry A. 2001;105: 9396–9409.
- [47] Soria FA, Zhang W, Paredes-Olivera PA, van Duin AC, Patrito EM. Si/C/H ReaxFF reactive potential for silicon surfaces grafted with organic molecules. The Journal of Physical Chemistry C. 2018;122: 23515–23527.
- [48] Plimpton S. Fast parallel algorithms for short-range molecular dynamics. Journal of Computational Physics. 1995;117: 1–19.
- [49] Ulman A. Formation and structure of self-assembled monolayers. Chemical Reviews. 1996;96: 1533–1554.
- [50] Ahmad K, Zhao X, Pan Y, Wang W, Huang Y. Atomic force microscopy measurement of slip on smooth hydrophobic surfaces and possible artifacts. The Journal of Physical Chemistry C. 2015;119: 12531–12537.
- [51] Bunker BC, CarPick RW, Assink RA, Thomas ML, Hankins MG, Voigt JA, Sipola D, de Boer MP, Gulley GL. The impact of solution agglomeration on the deposition of self-assembled monolayers. Langmuir. 2000;16: 7742–7751.
- [52] Chauhan A, Aswal D, Koiry S, Gupta S, Yakhmi J, Sürgers C, Gúerin D, Lenfant S, Vuillaume D. Self-assembly of the 3-aminopropyltrimethoxysilane multilayers on Si and hysteretic current–voltage characteristics. Applied Physics A. 2008;90: 581–589.
- [53] Ito E, Noh J, Hara M. Steric effects on adsorption and desorption behaviors of alkanethiol self-assembled monolayers on Au (111). Chemical Physics Letters. 2008;462: 209–212.
- [54] Hayashi T, Wakamatsu K, Ito E, Hara M. Effect of steric hindrance on desorption processes of alkanethiols on Au (111). The Journal of Physical Chemistry C. 2009;113: 18795–18799.
- [55] Houston JE, Kim HI. Adhesion, friction, and mechanical properties of functionalized alkanethiol self-assembled monolayers. Accounts of Chemical Research. 2002;35: 547–553.
- [56] Ramin L, Jabbarzadeh A. Frictional properties of two alkanethiol self assembled monolayers in sliding contact: Odd-even effects. The Journal of Chemical Physics. 2012;137.
- [57] Ahmad K, Yang Q, Martini A. Simulations of friction anisotropy on self-assembled monolayers in water. Langmuir. 2022;38: 6273–6280.
- [58] Kiely J, Houston J, Mulder J, Hsung R, Zhu X-Y. Adhesion, deformation and friction for self-assembled monolayers on Au and Si surfaces. Tribology Letters. 1999;7: 103–107.
- [59] Kim SH, Asay DB, Dugger MT. Nanotribology and MEMS. Nano Today. 2007;2: 22–29.
- [60] Rusu F, Pustan M, Bîrleanu C, Müller R, Voicu R, Baracu A. Analysis of the surface effects on adhesion in MEMS structures. Applied Surface Science. 2015;358: 634–640.

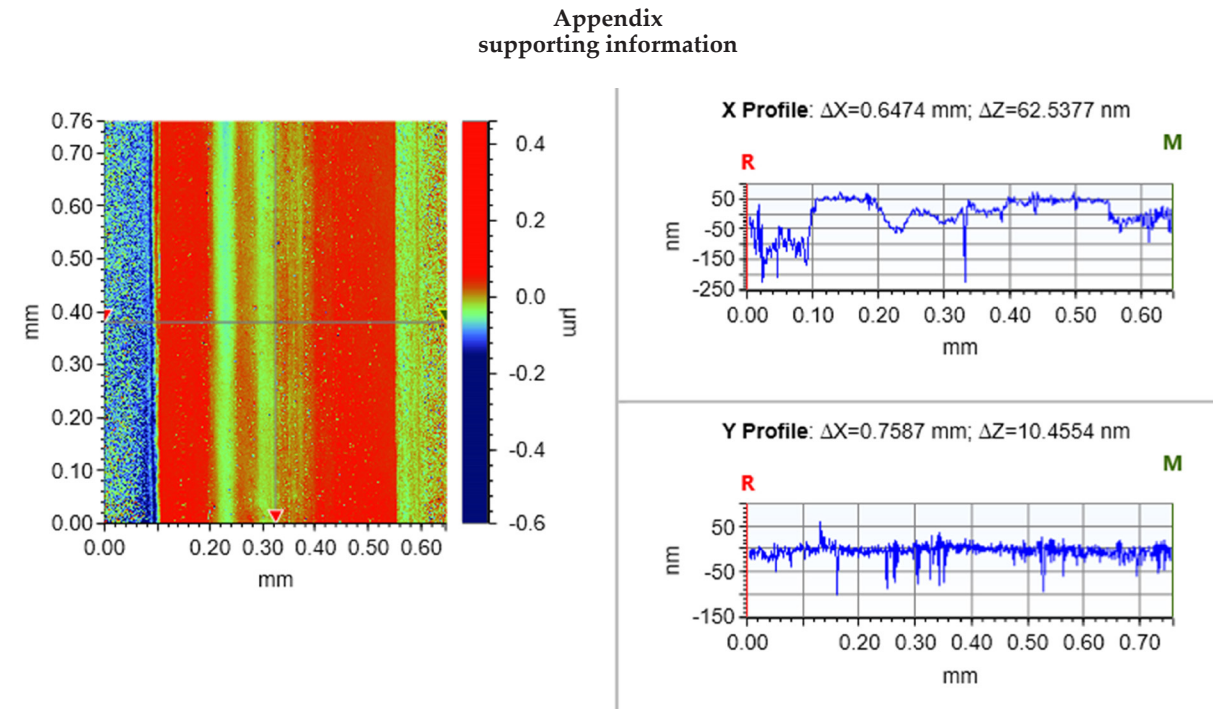


Fig. A1 Surface image of APTES wear track. The X and Y profiles show the line profiles the x direction (cross-section) and y direction (parallel to sliding). The profiles clearly suggest a film build-up of around 100 nm.

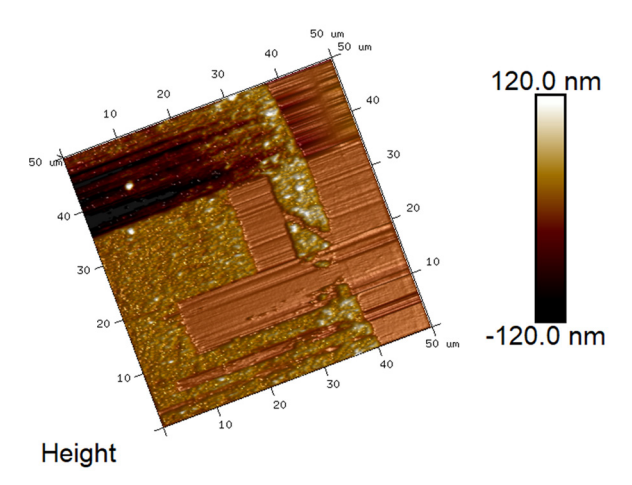


Fig. A2 Surface image of APTES wear track obtained through AFM

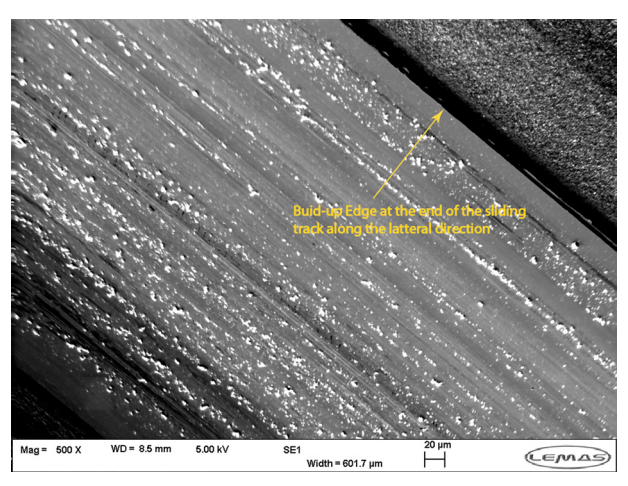


Fig. A3 SEM image of the APTES tribofilm, showing a clear build-up edge at the end of the sliding track in the lateral direction

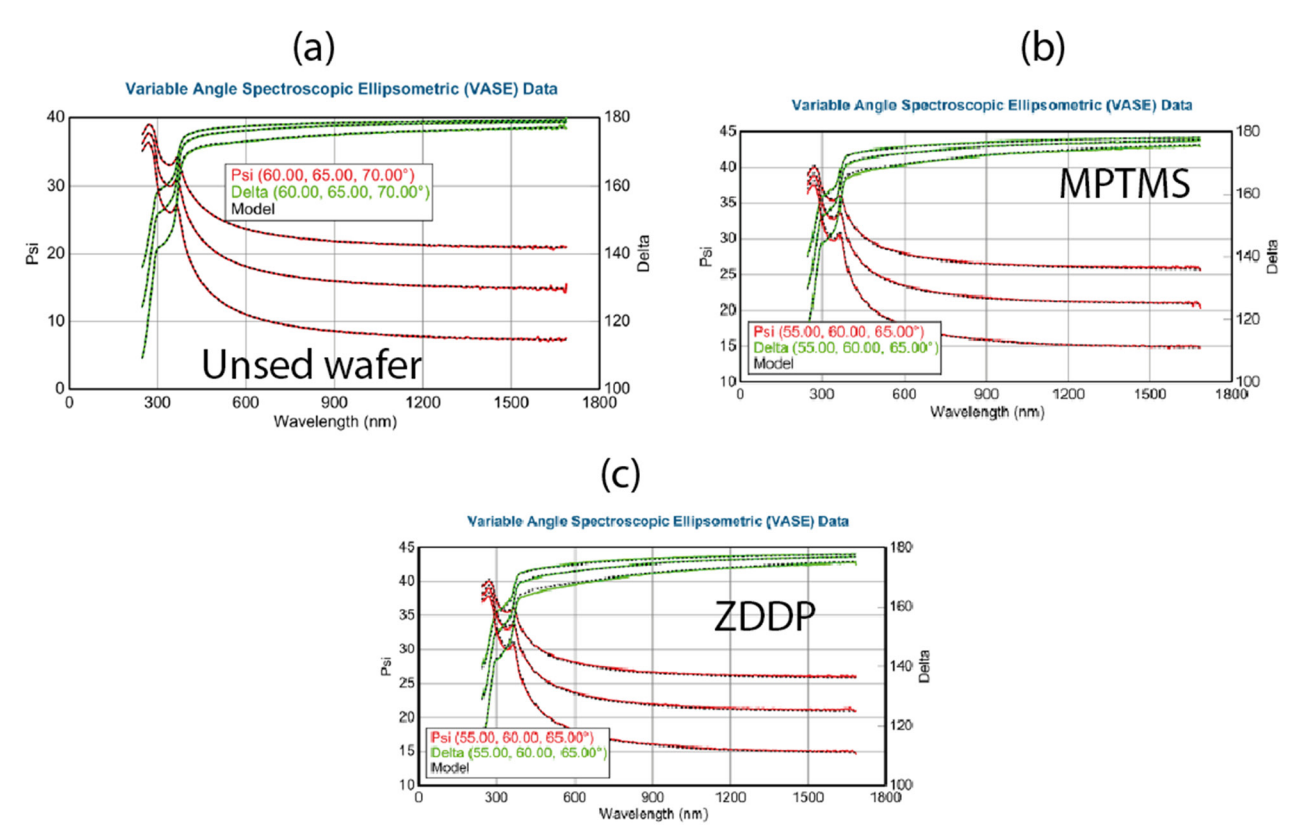


Fig. A4 Variable angle spectroscopic ellipsometric data curves for (a) unused silicon wafer (b) tribofilms of MPTMS and (c) ZDDP

The ellipsometry data was taken with 27 mm micro-optics installed and focused spot (elliptical) had a short axis width of 80 μ m. Issues such as back reflection were eliminated through the numerical aperture of focusing optics.

The psi-delta data was fitted with a film of constant RI (wavelength invariant) and roughness. The data fit suggested a thin film of 0.8 nm for the ZDDP and 0.9 nm for the MPTMS. The fitted data of the uncoated silicon sample suggested the presence of an oxide layer, as expected.

CC (1) (S) (E)

This paper is licensed under the Creative Commons Attribution-NonCommercial-NoDerivatives 4.0 International (CC BY-NC-ND 4.0) License. This allows users to copy and distribute the paper, only upon conditions that (i) users do not copy or distribute such paper for commercial purposes, (ii) users do not change, modify or edit such paper in any way, (iii) users give

appropriate credit (with a link to the formal publication through the relevant DOI (Digital Object Identifier)) and provide a link to this license, and (iv) users acknowledge and agree that users and their use of such paper are not connected with, or sponsored, endorsed, or granted official status by the Licensor (i.e. Japanese Society of Tribologists). To view this license, go to https://creativecommons.org/licenses/by-nc-nd/4.0/. Be noted that the third-party materials in this article are not included in the Creative Commons license, if indicated on the material's credit line. The users must obtain the permission of the copyright holder and use the third-party materials in accordance with the rule specified by the copyright holder.